The Spine Journal 23 (2023) 1435–1450

Systematic Review/Meta-Analysis

Innovative quantitative magnetic resonance tools to detect early intervertebral disc degeneration changes: a systematic review

Fabrizio Russo, MD, PhD[a,b], Luca Ambrosio, MD*[,a,b], Eugenio Giannarelli, MD[a], Ferruccio Vorini, MD[a,b], Carlo A. Mallio, MD, PhD[c,d], Carlo C. Quattrocchi, MD, PhD[c,d], Gianluca Vadalà, MD, PhD[a,b], Rocco Papalia, MD, PhD[a,b], Vincenzo Denaro, MD[b]

[a] *Department of Orthopaedic and Trauma Surgery, Research Unit of Orthopaedic and Trauma Surgery, Università Campus Bio-Medico di Roma, Rome, Italy*

[b] *Operative Research Unit of Orthopaedic and Trauma Surgery, Fondazione Policlinico Universitario Campus Bio-Medico, Rome, Italy*

[c] *Department of Diagnostic Imaging and Interventional Radiology, Research Unit of Diagnostic Imaging and Interventional Radiology, Università Campus Bio-Medico di Roma, Rome, Italy*

[d] *Operative Research Unit of Diagnostic Imaging and Interventional Radiology, Fondazione Policlinico Universitario Campus Bio-Medico, Rome, Italy*

Received 25 January 2023; revised 25 April 2023; accepted 16 May 2023

Abstract

BACKGROUND CONTEXT: Low back pain (LBP) is the leading cause of disability worldwide, with a tremendous socioeconomic burden. It is mainly caused by intervertebral disc degeneration (IDD), a progressive and age-related process. Due to its ability to accurately characterize intervertebral disc morphology, magnetic resonance imaging (MRI) has been established as one of the most valuable tools in diagnosing IDD. Innovative quantitative MRI (qMRI) techniques able to detect the earliest signs of IDD have been increasingly reported.

PURPOSE: To systematically review available reports on the application of novel qMRI techniques to detect early IDD changes.

STUDY DESIGN: Systematic literature review.

METHODS: A systematic search of PubMed/MEDLINE, Scopus, CINAHL, EMBASE, CENTRAL and Cochrane databases was performed through January 21, 2023. Randomized and nonrandomized studies on innovative qMRI tools able to diagnose early biochemical and architectural IDD changes in patients with or without discogenic LBP were searched. Data on study population, follow-up time (when applicable) and MRI sequence used were recorded. The QUADAS-2 tool was utilized to assess the risk of bias of included studies.

RESULTS: A total of 39 articles published between 2005 and 2022 resulted from the search. All novel qMRI techniques showed an increased capacity to detect early IDD changes thanks to the ability to assess subtle alterations of water content, proteoglycan and glycosaminoglycan concentration, and increased levels of catabolic biomarkers compared to conventional MRI.

CONCLUSIONS: Innovative qMRI techniques have proven effective in identifying premature IDD changes. Further studies are needed to validate their application in wider populations and confirm their applicability in the clinical setting.

Keywords: Diagnosis; Intervertebral disc; Intervertebral disc degeneration; Low back pain; Magnetic resonance imaging; Spectroscopy

FDA device/drug status: Not applicable.

Author disclosures: ***FR***: Nothing to disclose. ***LA***: Nothing to disclose. ***EG***: Nothing to disclose. ***FV***: Nothing to disclose. ***CAM***: Nothing to disclose. ***CCQ***: Nothing to disclose. ***GV***: Nothing to disclose. ***RP***: Nothing to disclose. ***VD***: Nothing to disclose.

*Corresponding author: Department of Orthopaedic and Trauma Surgery, Campus Bio-Medico University Hospital Foundation, Via Alvaro del Portillo 200, 00128; Rome, Italy. Tel.: +(39) 06 225418825.

E-mail address: l.ambrosio@unicampus.it (L. Ambrosio).

https://doi.org/10.1016/j.spinee.2023.05.011

Introduction

Low back pain (LBP) is a pandemic condition affecting more than 7.5% of the world population and the leading cause of disability worldwide, prompting a huge medical burden and immense economic costs for healthcare systems and societies [1]. Intervertebral disc degeneration (IDD) underlies most cases of LBP and is characterized by a plethora of alterations that irreversibly disrupt the intervertebral disc (IVD) structure and function [2]. These are mainly represented by progressive nucleus pulposus (NP) dehydration, development of annulus fibrosus (AF) tears, and reduction of disc height. Eventually, IDD can be complicated by serious sequelae including disc herniation, spinal stenosis, and degenerative spondylolisthesis, with development of severe neurological deficits requiring surgical treatment [3].

Magnetic resonance imaging (MRI) is the most widely adopted technique to evaluate the IVD in both healthy and degenerative conditions. By assessing proton density, water content, and biochemical composition, MRI is able to depict disc hydration and morphological characteristics with the advantage of being radiation-free and allowing for multiplanar representation of vertebral and paravertebral tissues [4]. Routine MRI sequences include axial T2-weighted, sagittal T1-weighted spin-echo, and T2-weighted spin-echo images. In T2-weighted sagittal images, normal IVDs display a hyperintense signal within the NP and the inner AF, while the outer AF is typically hypointense. With the onset of IDD, a progressive decrease of the NP T2-weighted signal with loss of disc height can be noted, along with additional alterations occurring at later stages. However, it has been demonstrated that these changes are present within the IVD when a substantial part of the degenerative process has already irreversibly taken place [5].

In the last decades, a growing number of innovative quantitative MRI (qMRI) techniques able to capture IDD at its earliest stages have been investigated. These groundbreaking technologies have demonstrated to identify premature IDD features including initial loss of proteoglycans (PG), glycosaminoglycans (GAG) and water content, end plate changes, identification of tissue biomarkers, change of physiological molecule distribution and fatty infiltration within both paravertebral muscles and vertebral bodies [4].

The aim of this study was to systematically review the available evidence on novel qMRI techniques for the identification of IDD to prompt an early diagnosis, optimize the treatment of related LBP and prevent its sequelae.

Materials and methods

A systematic search of PubMed/MEDLINE, Scopus, CINAHL, EMBASE, CENTRAL, and Cochrane databases was performed for literature published from inception to January 21, 2023. Briefly, we sought to identify studies concerning innovative qMRI tools able to diagnose early biochemical and architectural IVD degenerative changes in patients with or without discogenic LBP. The Preferred Reporting Items for Systematic reviews and Meta-Analyses (PRISMA) guidelines were used to improve the reporting of the review [6].

Inclusion and exclusion criteria

We included in our research randomized control trials and nonrandomized controlled studies such as prospective (PS) or retrospective cohort studies, case-series, case-control (C-C) and cross-sectional (C-S) studies with ≥10 patients included. Only studies in humans with abstracts written in English were considered, with no other limits placed on the search. Case reports, letters to editors, technical notes, instructional courses, preclinical studies, cadaveric investigations, systematic reviews, and meta-analyses were excluded, as well as studies evaluating the cervical or thoracic spine, or focusing on other causes of nondiscogenic LBP, such as osteoporosis, trauma, infection, cancer, or non-spinal diseases.

Search strategy

Keywords used in the search strategy included “low back pain,” “disc degeneration,” “spectroscopy,” “T2 mapping,” “T1ρ,” “T2 star”, “DWI,” “DTI,” “delayed gadolinium-enhanced MRI,” “GagCEST imaging,” “magnetization transfer ratio mapping,” “sodium magnetic resonance imaging” and “UTE”. The keywords were used isolated or combined. The definitive search string was composed as follows: “((low back pain) OR (disc degeneration)) AND ((((((((((spectroscopy) OR (T2 mapping)) OR (T1ρ)) OR (T2 star)) OR (DWI)) OR (DTI)) OR (delayed gadolinium-enhanced MRI)) OR (GagCEST imaging)) OR (magnetization transfer ratio mapping)) OR (sodium magnetic resonance imaging)) OR (UTE)).”

Study selection

The initial search of the articles was conducted by two reviewers (E.G. and L.A). In case of disagreements, the consensus of a third reviewer (F.R.) was asked. After removing duplicates, titles, and abstracts were independently screened by the two reviewers. Subsequently, if a paper was considered potentially relevant with regards to inclusion and exclusion criteria, full texts were reviewed, for possible inclusion in the review. Disagreements about eligibility were resolved through discussion with a third reviewer (F.R.).

Data extraction

The following data were extracted from the studies selected: authors, year of publication, country, sample size, mean age, and MRI sequences used. In addition, results and conclusions of each study were reported.

Quality of evidence

The methodological quality of included studies was independently graded by two reviewers (L.A. and F.R.), and any disagreement was resolved by the intervention of a third reviewer (G.V.) Risks of bias and applicability of included studies were assessed using assessment criteria established by the Quality Assessment of Diagnostic Accuracy Studies (QUADAS-2) [7]. This tool is based on four domains: patient selection, index test, reference standard, and flow and timing. Each domain is evaluated in terms of risk of bias, and the first three domains are also assessed in terms of concerns regarding applicability.

Results

Study selection

A total of 610 studies were found. After duplicate removal, 487 studies were obtained. Of the 487 studies, 406 were excluded through title and abstract screening. Then, 81 full-text articles were screened. Out of these studies, 51 were excluded (reports not retrieved, n=3; nondiscogenic LBP, n=8; studies focused on cervical or thoracic spine, n=15; no English language, n=25). Nine additional studies were identified from hand searching bibliographies of included studies or identified systematic reviews. After this process, 39 articles were included in our review. The number of articles excluded or included were registered and reported in a PRISMA flowchart (Fig. 1). The high heterogeneity among studies (in terms of MRI sequences used, patients' characteristics and outcome measures) precluded and effective meta-analysis from being performed.

Study characteristics

Selected studies included 1 PS [8], 11 CC [9−19] and 27 C-S [20−45]. Studies were published between 2005 [20] and 2022 [41]. As most studies were composed of CC and C-S, no follow-up was reported except for the only PS (Table 1) [8]. qMRI sequences used included T1ρ (18 studies [10,11,16,18-21,23,27,32,35,37-41,45,46]), T2* (7 studies [22,29,34,35,37,38,41]), T1 mapping with gadolinium enhancement (1 study [24]), T2 mapping (17 studies [11,15,17,18,21,23,25,26,30,31,33,34,38,41,44-46]), DWI (3 studies [11,29,35]), DTI (2 studies [17,29]), UTE (7 studies [9,27,36,40,42,43,45]), gagCEST (5 studies [13,28,32,35,47]), magnetic resonance spectroscopy (MRS; 2 studies [8,19]), Iterative Decomposition of water and fat with Echo Asymmetry and Least-Squares Estimation (IDEAL, 2 studies [9,46]), ^{23}Na-MRI (2 studies [14,25]) and chemical shift encoding-based water-fat MRI (CSE-MRI, 1 study [40]).

Risk of bias

The QUADAS-2 tool was utilized to assess the risk of bias of each study. Thirty-four studies were rated on a three-point scale, reflecting concerns about risk of bias and applicability as low, unclear, or high, as shown in Fig. 2 (details of the analysis are presented in Supplementary Data).

Results of individual studies

MRI sequence characteristics with corresponding outcomes and conclusions of included studies are summarized in Table 2. Most studies investigated multiple sequences together; therefore, their results have been grouped per MRI sequence and discussed below. An overall summary of specific features and advantages of qMRI tools described over traditional MRI is depicted in Table 3.

T1ρ

In included studies, T1ρ was performed in both healthy patients and individuals affected by LBP. In the former population, T1ρ relaxation times of lumbar IVDs significantly correlated with the Pfirrmann score evaluated with conventional sagittal T2-weighted imaging [20], but were not associated with either sex or body mass index (BMI) [23,39]. Interestingly, in young asymptomatic subjects, T1ρ values within the NP were significantly higher than those in the AF at all levels, and progressively decreased from L1 to S1. Furthermore, T1ρ values were significantly lower in L3 to L4 and L4 to L5 NP and L3 to L4 AF of women compared to men [16,39].

In patients affected by LBP, T1ρ values were significantly lower in both the NP and AF compared to healthy peers and were negatively correlated with Pfirrmann scores [11], especially at intermediate grades (2−4). Indeed, the variability of T1ρ values was significantly higher at lower grades, stabilized at intermediate degrees, and then increased again in severely degenerated IVDs. Likewise, texture parameters such as dissimilarity and contrast sharply decreased with degeneration at early stages before increasing again at later stages of IDD [26,32,35,37,41,45]. Intriguingly, in patients with LBP receiving provocative discography (PD), painful IVDs showed significantly lower T1ρ relaxation times compared to nonpainful discs [10,19]. Lower T1ρ values have also been significantly associated with worse outcomes in terms of Oswestry Disability Index (ODI), Short Form (SF)-36, and visual analog scale (VAS) [19,21,46] as well as with age, but only in LBP patients [23,40]. Furthermore, reduced IVD T1ρ relaxation times were also correlated with T1ρ in facet joint cartilage [38], cartilaginous end plate (CEP) T2* values, and vertebral bone marrow fat fraction (BMFF), which is inversely proportional to the amount of hematopoietic marrow and thus an indicator of IVD perfusion [40,46]. Moreover, T1ρ also showed appreciable reliability in successfully detecting disc bulging, herniations, and high-intensity zones (HIZs) within the AF [41].

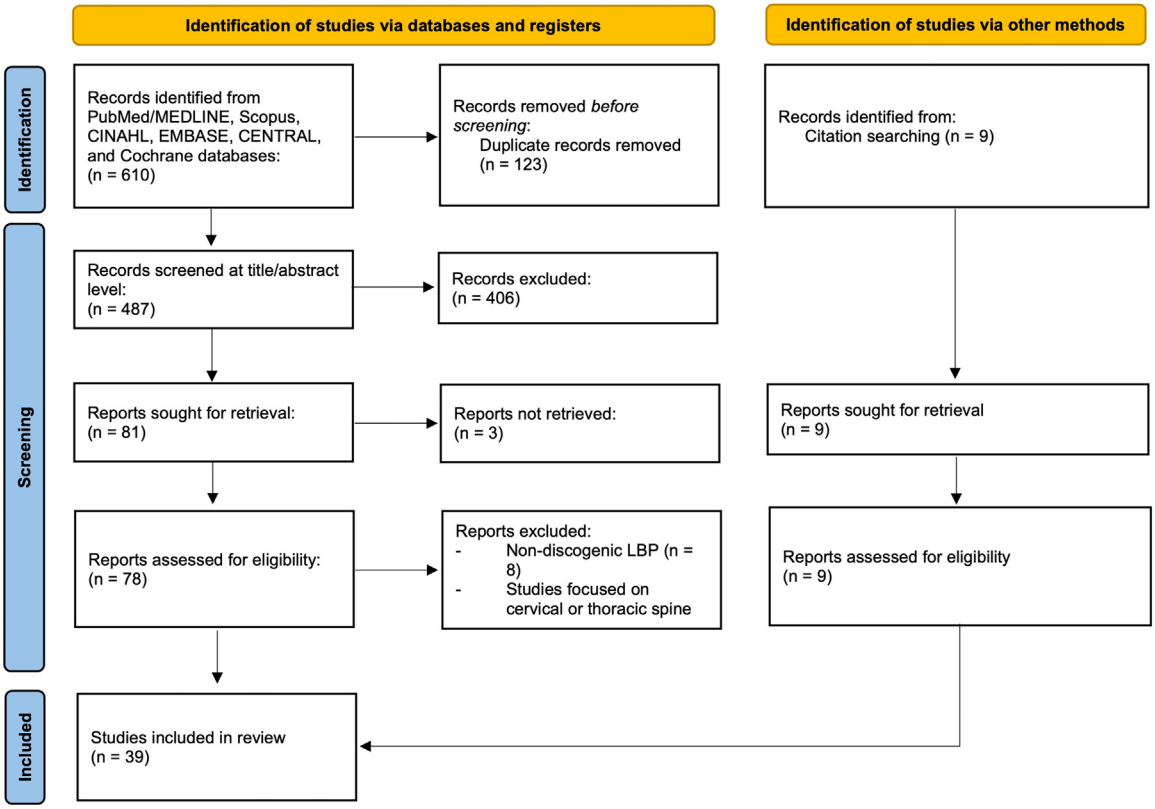

Fig. 1. Search strategy flow diagram in accordance with the Preferred Reporting Items for Systematic Reviews and Meta-Analyses (PRISMA) protocol.

*T2**

In healthy IVDs, due to different biochemical composition, T2* values were reported to be higher in the NP compared to the AF and progressively increased from L1 to S1 [29]. In patients with LBP, NP T2* relaxation times were significantly lower, whereas signal differences could be detected with less sensitivity in the outer AF region due to the lower water content [22]. T2* values within the NP, AF and facet joint cartilage notably decreased with worsening IDD as per the Pfirrmann score [38,45], with a higher degree of accuracy especially at intermediate grades [35,37,41,42]. Indeed, with advancing IDD, due to progressive disc dehydration, the overall drop of T2* values rendered individual IVD regions less distinguishable as a consequence of decreased spatial differentiation [34]. Furthermore, T2* relaxation times were significantly lower in bulging/herniated IVDs and in presence of HIZs compared to normal IVDs [41].

T1 mapping with gadolinium enhancement

Niinimaki et al. [24] performed T1 imaging with gadolinium enhancement of healthy IVDs. NP T1 relaxation time significantly decreased following paramagnetic contrast administration. A statistically significant difference in T1 relaxation rates, both pre- and postcontrast, was reported among all Pfirrmann grades except for grades four and five. Moreover, the mean change of T1 values was significantly correlated with disc height.

T2 mapping

According to reviewed studies, T2 relaxation times progressively decreased with increasing age and Pfirrmann score [17,18,21,25,33], while being positively correlated with disc volume [23]. On the other hand, no association with sex was reported [23]. Due to the higher water content, changes were more frequently evident and significant in the NP compared to the AF, especially in the setting of mild IDD, with healthy and severely degenerated IVDs showing less spatial differentiation [26,30,31,34,38,45]. Interestingly, T2 mapping tended to classify Pfirrmann 1 IVDs with a higher grade, due to the capacity to detect earlier subtle degenerative changes that could not be noticed using conventional T2 imaging [33]. T2 mapping revealed significantly lower values in subjects with LBP, disc bulging or herniation, and HIZs compared to asymptomatic individuals [11,17,41], with a higher discrimination sensitivity than T1ρ and T2* mapping [41]. Furthermore, lower T2 values were also significantly correlated with vertebral BMFF as well as with poorer ODI, VAS and Japanese Orthopedic Association Back Pain Evaluation Questionnaire (JOABPEQ) outcomes [15,46]. In the study from Lagerstrand et al. [44], T2 mapping was performed on LBP patients after spinal axial loading. T2 values were significantly

Table 1
Study design and patient demographics of included studies

Study	Country	Study design	Sample size (n)		Mean age (years)	
Auerbach [20]	USA	Cross-sectional	10 (healthy)		40−60	
Bailey [9]	USA	Case-control	38 (LBP)	14 (no LBP)	47.9±12.6 (LBP)	45.7±12.3 (no LBP)
Blumenkrantz [21]	USA	Cross-sectional	10 (LBP)	6 (no LBP)	40.2±12.4	
Bonnheim [40]	USA	Cross-sectional	84 (LBP)		40.0±11.9	
Borthakur [10]	USA	Case-control	17 (LBP)	11 (no LBP)	44±6 (LBP)	43±17 (no LBP)
Cui [11]	China	Case-control	30 (LDH); 30 (LBP)	30 (no LBP)	58.2±14.3 (LDH); 56.9±12.8 (LBP)	57.6±12.5 (no LBP)
Deng [12]	China	Case-control	13 (LBP)	12 (no LBP)	59.1 (LBP)	30.3 (no LBP)
Frenken [13]	Germany	Case-control	18 (LDH); 16 (LBP)	20 (no LBP)	57.5±22.5 (LDH); 59±17.5 (LBP)	54.5±11.5 (no LBP)
Gornet [8]	USA	Prospective	139 (LBP)		41	
Haneder [14]	Germany	Case-control	12 (LBP)	55 (no LBP)	35.3 (LBP);	28.8 (no LBP)
Hoppe [22]	Switzerland	Cross-sectional	93 (LBP)		53±16	
Lagerstrand [44]	Sweden	Cross-sectional	26 (LBP)		28 (25−69)	
Krug [46]	USA	Cross-sectional	37 (LBP)	9 (no LBP)	47.3±12.0	
Menezes-Reis [23]	Brazil	Cross-sectional	90 (healthy)		27.1±4.8	
Niinimaki [24]	Finland	Cross-sectional	20 (healthy)		49	
Noebauer-Huhmann [25]	Austria	Cross-Sectional	10 (healthy)		30±7	
Ogon [15]	Japan	Case-control	28 (LBP)	25 (no LBP)	48.9±9.6 (LBP)	43.8±14.5 (no LBP)
Pandit [26]	USA	Cross-sectional	16 (LBP)		48.12±14.08	
Pang [27]	China	Cross-sectional	108		52±7.7	
Schleich [28]	Germany	Cross-sectional	48 (healthy)		31±8	
Shen [29]	China	Cross-sectional	40 (healthy)		24.35±1.8	
Stelzeneder [30]	Austria	Cross-sectional	66 (LBP)		38.8±11.2	
Takashima [31]	Japan	Cross- sectional	60 (LBP)		53.3	
Takashima [45]	Japan	Cross- sectional	55 (LBP)		56±21.3	
Togao [32]	Japan	Cross- sectional	24		36.0±8.5	
Vadalà [16]	Italy	Case-control	13 (No LBP weightlifters)	13 (No LBP sedentary)	25.3±4.4 (No LBP weightlifters)	23.5±1.3 (No LBP sedentary)
Vadapalli [17]	India	Case-control	59 (LBP)	59 (No LBP)	41.7±11.80	
Wang [18]	China	Case-control	40 (LBP)	12 (No LBP)	54.1 (LBP)	32.1 (No LBP)
Watanabe [33]	Switzerland	Cross-sectional	29 (healthy)		31.8±8.1	
Wei [43]	China, USA	Cross-sectional	17		43±16	
Welsch [34]	Austria	Cross-sectional	30 (LBP)		38.1±9.1	
Wu [42]	China	Cross-sectional	76 (LBP)		54.5±15.7	
Xiong [35]	China	Cross-sectional	37 (LBP)		48.3	
Yang [41]	China	Cross-sectional	39 (LBP)		44 (22−80)*	
Zehra [36]	China	Cross-sectional	106		52.3	
Zhang [37]	China	Cross- sectional	42 (LBP)		44.2	
Zhang [38]	China	Cross- sectional	22 (LBP)		33.2	
Zobel [39]	Italy	Cross-sectional	63 (No LBP)		22.95±1.8	
Zuo [19]	USA	Case-control	26 (LBP)	23 (No LBP)	44.8±8.7 (LBP)	35.1±12.6 (No LBP)

* Median age and age range.LBP, low back pain; LDH, lumbar disc herniation.

lower in the presence of HIZs, end plate changes, and Modic changes. Furthermore, NP T2 values considerably changed after loading when associated with concomitant endplate changes.

Diffusion imaging

In healthy subjects, DWI and DTI showed a significant gradual reduction of apparent diffusion coefficient (ADC) from the NP to the AF, while fractional anisotropy (FA) values increased from the periphery towards the center of the IVD. Furthermore, mean ADC and FA values progressively increased from L1−L2 to L5−S1 [11,29] and, differently from individuals with LBP, were significantly associated with age [17]. Predictably, patients with LBP or disc herniation showed lower ADC values compared to asymptomatic peers. Furthermore, ADC values in both the NP and AF progressively decreased with advancing Pfirrmann grades, with all between-group differences being significant [35].

UTE

Bailey et al. [9] acquired UTE sequences to analyze CEPs in patients with chronic LBP and matched asymptomatic individuals. Authors found that CEP damage, Modic changes and mean Pfirrmann grade were independent predictors of chronic LBP. UTE was also performed to analyze CEP composition in the study by Bonnheim and colleagues [40]. The authors found that CEP T2* was independently and significantly associated with NP T1ρ and age, and able to predict NP T1ρ values in the multivariate model. Pang and colleagues [27] investigated the association between IDD and the UTE disc sign (UDS), described as a hypo- or hyperintense band within the disc at UTE sequences, in a population-based cohort. UDS was noted in 13.1% of segments and significantly associated with multilevel and moderate/severe IDD, disc bulges/extrusions, Modic changes, spondylolisthesis, and lower T1ρ values in the same IVD. Moreover, UDS was significantly correlated with the occurrence of chronic

Table 2
MRI sequences, results, and conclusions of included studies

Study	MRI sequence	Results	Conclusions
Auerbach [20]	T1ρ	T1ρ significantly correlated with Pfirrmann grade (r=−0.51, p<.01).	T1ρ has a strong potential as a non-invasive biomarker of PG loss and early IDD.
Bailey [9]	UTE, IDEAL	CEP damage (OR: 14.1, 95%CI: 2.3−85.2, p<.01), any MC (OR: 5.4, 95%CI: 1.1−27.5, p=.04), and mean Pfirrmann grade (OR: 5.2, 95%CI: 1.4−18.9, p<.01) were predictors of CLBP. Patients with a high ODI score (>40) showed significantly greater MF FF values than controls. CEP damage at L4-L5 was predictive of CLBP in patients with higher PSM FF values (p<.05).	The relationship between reduced PSM quality and endplate defects may be predictive of CLBP.
Blumenkrantz [21]	T1ρ, T2 mapping	T1ρ and T2 progressively decreased with increasing Pfirrmann grade and were significantly associated between each other (p<.05). T1ρ was also associated with ODI, SF-36 (p<.05) and patients' age (p<.01).	T1ρ and T2 decrease with increasing grade of IDD and T1ρ values were related to clinical symptoms.
Bonnheim [40]	T1ρ, CSE-MRI, UTE	CEP T2* and vertebral BMFF were independently significantly associated with NP T1ρ (p<.001), although after adjusting for age, sex, and BMI the correlation with BMFF was lost. However, NP T1ρ was negatively associated with age and Pfirrmann grade (p<.0001).	Poor CEP composition correlates with IDD independently of vertebral vascularity.
Borthakur [10]	T1ρ	T1ρ was significantly lower in painful IVDs of LBP patients vs controls (p<.001) and was correlated with the Pfirrmann score (r=−0.52, p<.001).	T1ρ is a quantitative measure of IDD and may serve as a reliable biomarker.
Cui [11]	T1ρ, T2 mapping, DWI	T1ρ, T2 and ADC highest values in both NP and AF were found in asymptomatic patients, while they were lower in subjects with LDH compared to IDD (p<.05).	T1ρ, T2 mapping and DWI may improve IDD diagnostic accuracy.
Deng [12]	gagCEST	gagCEST values decreased with advancing IDD (p<.001) and were significantly correlated with Pfirrmann grading both in the NP and AF (p<.05).	gagCEST can detect IDD with a higher accuracy compared to T2, especially in the AF.
Frenken 2021 [13]	gagCEST	gagCEST values were higher in the NP than in the AF (p<.001) and in Pfirrmann grades ≤2 compared to grades ≥3 (p<.001), while being lower in patients with LBP compared to individuals with radiculopathy or no LBP.	GAG depletion in LBP and in IVDs adjacent to extrusions indicate close interrelatedness of structural IVD changes in IDD.
Gornet [8]	MRS	MRS was able to predict painful IVDs at PD and the degree of IDD when Pfirrmann grading was >2. In patients undergoing surgery, when all MRS-positive IVDs were treated, success rate was 97% versus 57% when the treated level was MRS-negative.	MRS correlates with PD and may support improved surgical outcomes for CLBP patients.
Haneder [14]	^{23}Na-MRI	^{23}Na was significantly reduced in degenerated IVDs (Pfirrmann scores 4−5; p<.001). No statistically significant differences were seen among IVDs with the same Pfirrmann score. Mean ^{23}Na was significantly greater in healthy women compared to healthy men (p<.001).	^{23}Na-MRI is a noninvasive, independent, in vivo predictor/biomarker of IDD.
Hoppe 2012 [22]	T2*	T2* values were significantly lower in degenerated IVDs due to decreased NP water content (p<.05).	Axial T2* mapping is a quantitative and effective tool to detect early stages of IDD.
Krug [46]	IDEAL, T1ρ, T2 mapping	A significant association was found between vertebral BMFF and T1ρ/T2 (p<.05); T1ρ/T2 were also significantly associated with VAS, ODI and Pfirrman grading (p<.001), while BMF was significantly associated with both ODI and VAS.	BMFF is strictly correlated with biochemical changes within the IVD and may predict premature disc dehydration.

Table 2 (***Continued***)

Study	MRI sequence	Results	Conclusions
Lagerstrand [44]	T2 mapping	T2 values were lower in IVDs showing concomitant HIZs, endplate changes and Modic changes.	T2 mapping effectively reflects spinal changes associated with HIZs, Modic changes and endplate changes.
Menezes-Reis [23]	T1ρ and T2 mapping	There was a negative correlation between age and IVD T2 relaxation time (r=−0.30, p<.001) and a positive correlation with disc volume (r=0.15, p=.002).	T2 relaxometry identified gradual disc dehydration related to aging, while T1ρ did not show significant correlations with age.
Niinimaki [24]	T1-Gd enhanced mapping	A statistically significant decrease in NP T1 relaxation time was observed following Gd intake (p<.0001) in all Pfirrmann grades, with significant intergroup differences (p<.05) except between four and five. T1 mean change was also associated with disc height (R^2=0.458, p<.001).	Quantification of delayed enhancement of the IVD may provide new insights into IDD.
Noebauer-Huhmann [25]	^{23}Na-MRI, T2 mapping	The Pearson correlation coefficient showed a cubic function between ^{23}Na-MRI and modified Pfirrmann score, an inverse correlation between T2 mapping and modified Pfirrmann score (r=−0.62; p<.001), and no correlation between ^{23}Na-MRI and T2 mapping.	^{23}Na-MRI and T2 mapping can help characterize IDD changes related to the Pfirrmann score.
Ogon [15]	T2 mapping	T2 values were significantly lower in the PAF (p<.01) and were associated with poorer VAS (p<.01) and JOABPEQ scores (p<.05).	T2 mapping may provide an estimate of discogenic LBP due to degeneration of the PAF.
Pandit [26]	T1ρ and T2 mapping	T1ρ and T2 values decreased with increasing grade of NP degeneration (p<.05). Standard deviation of T1ρ and T2 values, as well as contrast and dissimilarity, steeply decreased at lower grades of IDD and later increased at advanced stages.	T1ρ and T2 relaxation times in the NP decrease with IDD severity.
Pang [27]	UTE, T1ρ	UDS was associated with IDD extent and severity (p<.01), MCs (p<.001), spondylolisthesis (p<.01) and lower T1ρ values (p<.05). The UDS score significantly correlated with worse ODI scores and LBP (p<.01), whereas T2W did not.	UDS is a novel imaging biomarker that is highly associated with degenerative spine changes, CLBP and disability than conventional T2 MRI.
Schleich [28]	gagCEST	NP gagCEST values demonstrated a significant negative correlation with morphological Pfirrmann score (NP: r=−0.562, p<.0001; AF: r=−0.444, p<.0001). The MTR_{asym} values were higher in nondegenerative lumbar IVDs (Pfirrmann 1−2) compared with degenerative IVDs (p<.001). NP MTR_{asym} values were significantly higher in normal appearing discs compared with herniated IVDs (p<.001).	gagCEST may be a powerful, non-invasive tool to investigate early IDD and therapy effects on GAG content.
Shen [29]	DWI, DTI, T2*	ADC and T2* values significantly decreased from the NP to the AF (p<.05), while FA values showed the opposite tendency. ADC, T2* and FA values increased from L1−L2 to L5−S1 (p<.05).	ADC, FA and T2* values may quantitatively reflect the microstructural characteristics of NP in early IDD.
Stelzeneder [30]	T2 mapping	NP T2 values showed a stepwise decrease from Pfirrmann grade 1 to 4 (p<.001). PAF showed the highest T2 values in Pfirrmann grade 2, while AAF showed relatively constant T2 values in all Pfirrmann grades.	T2 mapping may quantitatively characterize different degrees of IDD.
Takashima [31]	T2 mapping	T2 values significantly decreased in the NP from Pfirrmann grade 1 to 4 (p<.01). No significant difference was found in the AF area.	T2 value decreases with increasing IDD likely reflects a decrease in PG and water content in the NP.
Takashima [45]	T1ρ, T2 and T2* mapping	T1ρ, T2 and T2* values significantly decreased with increasing Pfirrmann grading (p<.005), with T1ρ and T2 not showing considerable differences between Pfirrmann grade 4 vs 5.	Although T1ρ, T2 and T2* were all highly sensitive to IDD, T2* may be more accurate at later stages of IDD.
Togao [32]	gagCEST, T1ρ	T1ρ values progressively decreased with increasing Pfirrmann grade, with statistical	gagCEST could be a reliable and quantitative technique for assessing IDD.

Table 2 (***Continued***)

Study	MRI sequence	Results	Conclusions
		significance at each grade (p<.001) except between grades 3 vs 4 and 4 vs 5. T1ρ values showed the widest variability in Pfirrmann grade 1 (101.1−157.0 ms). gagCEST signal was negatively correlated with Pfirrmann grade (p<.001) and positively correlated with T1ρ (p<.01).	
Vadalà [16]	T1ρ	NP T1ρ values decreased from upper to lower lumbar levels in both sedentary and weight-lifters and were significantly lower in weight-lifters compared with controls.	T1ρ can be used to identify early changes in the IVD in individuals with lifestyle and environmental factors associated with IDD.
Vadapalli [17]	T2 mapping, DTI	T2 values decreased with age in both healthy and LBP patients (p<.001), while FA AF/NP ratio decreased with aging only in the control group (p<.001). T2 and AF/NP ratio were significantly higher in healthy individuals compared to LBP patients at any age (p<.001).	T2 mapping and DTI provides objective evidence of IDD and can help detect early degeneration.
Wang [18]	T1ρ and T2 mapping	T1ρ and T2 values significantly decreased more rapidly with aging in the NP compared to AF.	T1ρ and T2 mapping can effectively detect aging-related IDD changes.
Watanabe [33]	T2 mapping	T2 values decreased in the NP and increased in the AF with advancing IDD (p<.05). The ratio of IVDs classified as grade 1 was higher with the conventional classification systems than that with axial T2 mapping.	Axial T2 mapping may detect early degenerative changes before conventional classification systems.
Welsch [34]	T2* and T2 mapping	T2* and T2 mapping were able to discriminate IVD ROI spatial differentiation especially for ROIs including the NP (p<.05). Signal changes became more evident with increasing Pfirrmann grade.	T2 and T2* mapping are able to identify subtle biochemical changes in the parametric evaluation and quantification of IDD.
Wei [43]	T1ρ-UTE	T1ρ values in the NP, AF and CEPs were significantly correlated with each other as well as with Pfirrmann grading. T1ρ values showed a strong negative correlation with Pfirrmann scores (r=-0.94, p<.001) and age (r=−0.76, p<.001). Furthermore, T1ρ relaxation times were significantly lower in patients with LBP compared to asymptomatic subjects (p<.005).	T1ρ-UTE can identify subtle changes in all IVD tissues, providing a comprehensive assessment of IDD.
Wu [42]	T2* mapping and T2*-UTE	UTE-T2* (r=−0.733, p<.001) and T2* (r=−0.654, p<.001) negatively correlated with Pfirrmann grades, while the former demonstrated to better discriminate among Pfirrmann scores and to more accurately evaluate both early and advanced IDD.	UTE-T2* may be a promising tool to quantitively assess early IDD.
Xiong [35]	T2*, gagCEST, DWI, T1ρ	T2*, gagCEST, ADC and T1ρ values decreased significantly with increasing IDD (p<.001), with gagCEST showing the strongest correlation with Pfirrmann grades and the highest discriminant accuracy compared to other parameters both for NP (r=−0.951, p<.001) and AF (r=−0.938, p<.001).	gagCEST revealed an excellent negative correlation with the Pfirrmann grading compared to other parameters.
Yang [41]	T1ρ, T2 and T2* mapping	T1ρ, T2 and T2* mapping was able to identify IDD changes including disc bulging, herniation and annular tears (p<.005), although T2 mapping performing better in terms of detection of early degenerative changes (p<.001).	T2 mapping may be of great utility for detecting the early and later changes of IDD.
Zehra [36]	UTE	72.2% of subjects with disc calcification had corresponding UDS (p<.001). Both the number of calcified disc levels on plain radiographs and the number of UDS levels were also correlated to each other (r=0.58, p<.001).	Disc calcification was correlated with UDS, suggesting that it may represent disc calcification.
Zhang [37]	T1ρ and T2* mapping	T1ρ and T2* showed significant differences at intermediate Pfirrmann grades (2−4) in the NP (p<.001), while AF T1ρ reported significant differences from grades >2 and T2* from grades >1 (p<.001).	T1ρ and T2* values significantly and negatively correlate with the Pfirrmann grades of IDD.

Table 2 (***Continued***)

Study	MRI sequence	Results	Conclusions
Zhang [38]	T1ρ, T2 and T2* mapping	T1ρ, T2 and T2* NP values decreased with increasing IDD at Pfirrmann classification (p<.001). T1ρ values were significantly lower comparing grade 2 vs 3 and 3 vs 4 (p<.01). T2* values were significantly lower comparing grade 2 vs 3 in the PAF (p<.01). No significant change was noted in the AAF. T1ρ and T2* values in the LFJ cartilage decreased with advancing IDD and was correlated with T1ρ changes in the NP and PAF (p<.05).	T1ρ is more sensitive than T2 and T2* values for assessing early degenerative changes in the LFJ cartilage and showed that LFJ degeneration may be correlated with IDD.
Zobel [39]	T1ρ	NP T1ρ values were significantly higher than those of AF at all levels and decreased from L1 to S1 (p<.0001). T1ρ values were significantly lower in women at L3−L4 and L4−L5 NP and L3−L4 AF (p<.05). T1ρ were negatively correlated with Pfirrmann grades (p<.0001).	T1ρ values correlate with Pfirrmann degenerative grade in young adults and are able to identify early IDD.
Zuo [19]	MRS, T1ρ	T1ρ values were significantly lower in patients with LBP compared to controls (p<.05), but not among patients with either positive or negative PD. The water/PG peak area ratio was significantly more elevated in patients compared to controls (p<.05) and in PD-positive IVDs compared to PD-negative IVDs (p<.05). An increased water/PG peak area ratio and decreased T1ρ values were associated with worse outcomes at ODI and SF-36 (p<.05).	MRS-quantified water, PG and T1ρ may potentially serve as biomarkers of symptomatic IDD.

^{23}Na-MRI, sodium magnetic resonance imaging; AAF, anterior annulus fibrosus; ADC, apparent diffusion coefficient; AF, annulus fibrosus; BMFF, bone marrow fat fraction; CEP, cartilaginous end plate; CI, confidence interval; CLBP, chronic low back pain; CSE-MRI, chemical shift encoding-based water-fat MRI; DTI, diffusion tensor imaging; DWI, diffusion-weighted imaging; FA, fractional anisotropy; FF, fat fraction; gagCEST, glycosaminoglycan chemical exchange saturation transfer; Gd, gadolinium; IDD, intervertebral disc degeneration; IDEAL, Iterative Decomposition of water and fat with Echo Asymmetry and Least-Squares Estimation; IVD, intervertebral disc; JOABPEQ, Japanese Orthopaedic Association Back Pain Evaluation Questionnaire; LBP, low back pain; LDH, lumbar disc herniation; LFJ, lumbar facet joints; MC, Modic change; MF, multifidus; MRS, magnetic resonance spectroscopy; MTR_{asym}, magnetization transfer asymmetry ratio; NP, nucleus pulposus; ODI, Oswestry disability index; PAF, posterior annulus fibrosus; PD, provocative discography; PSM, paraspinal muscle; ROI, region of interest; UDS, ultrashort echo time disc sign; UTE, ultrashort echo time; VAS, visual analog scale.

LBP and worse ODI scores, whereas conventional T2 imaging was not. In a subsequent study, UDS was found to be associated with disc calcifications seen at X-rays in 72.3% of investigated segments and the number of calcified IVDs was positively associated with the number of UDS-positive IVDs. However, 27.6% of IVDs showing calcification were not positive for UDS, while 52.2% of UDS-positive IVDs did not reveal calcification on radiographs [36]. In their study, Wu and colleagues [42] demonstrated that T2*-UTE was correlated with Pfirrmann classification by displaying significant differences between each Pfirrmann grade and showing a remarkable accuracy in identifying early and advanced IDD signs in both the NP and AF. Wei et al. [43] performed UTE with adiabatic T1ρ preparation and showed that T1ρ values in the NP, AF and CEPs were significantly correlated with each other as well as with Pfirrmann grading and age. Furthermore, T1ρ relaxation times were significantly lower in patients with LBP compared to asymptomatic subjects.

gagCEST

According to included studies, gagCEST values were generally higher in the NP than in the AF, tended not to vary among different lumbar levels, and progressively decreased with advancing IDD [28]. Interestingly, gagCEST has been shown to significantly discriminate between single Pfirrmann grades with a higher sensitivity and at earlier stages compared to T2 sequences, which detected notable changes in both the NP and AF only at more advanced degrees of IDD [12,13,32,35]. In general, gagCEST values were lower in individuals with LBP or disc herniation compared to healthy controls [13,28], and showed the highest correlation with Pfirrmann grades and the highest discriminant accuracy compared to other methods (T2*, ADC and T1ρ) in both the NP and AF [35].

MRS

In their study, Zuo et al. [19] showed that the water/PG peak area ratio was positively associated with increasing

Table 3
Summary of specific features and advantages of qMRI tools described over traditional MRI

MRI sequence	Specific features	Advantages over traditional MRI	Relevant references
T1ρ	• Specifically tracks relaxation time changes of water bound to large macromolecules such as GAGs and PGs • Correlates with the degree of IDD, patient-reported outcomes, and composition of CEPs and LFJs • Lower values have been reported in painful IVDs at PD	• T1ρ can detect subtle IDD changes earlier than conventional T2-weighted imaging	[10,11,16,18–21,23,27,32,35,37–41,45,46]
T2*	• Yields biochemical information regarding the IVD ultrastructure with the additional benefit of three-dimensional acquisition • Able to detect advancing IDD and LFJ degeneration	• T2* provides higher spatial resolution and signal in a shorter scan time	[22,29,34,35,37,38,41]
T1-Gd enhanced mapping	• By diffusing into the IVD, Gd can shorten T1 relaxation time and describe IVD nutrient transfer kinetics • Higher Gd enhancement in severely degenerated IVDs may be explained by aberrant neovascularization and higher diffusivity due to reduced disc height	• T1-Gd enhanced mapping can provide additional information on nutrient kinetics and IVD architecture	[24]
T2 mapping	• Provides information about water content and extracellular matrix structure, reflecting the presence of edema and early dehydration • More accurate in highly hydrated tissues (ie, NP and CEPs) compared to the AF • Correlates with the degree of IDD and patient-reported outcomes	• T2 mapping provides a quantitative analysis compared to the qualitative assessment performed with traditional T2-weighted MRI	[11,15,17,18,21,23,25,26,30,31,33,34,38,41,44–46]
DWI/DTI	• Reflect microstructural changes within the IVD based on water diffusion • DWI analyzes the overall capacity of water diffusion thus describing tissue hydration • DTI assesses the directional characteristics of water diffusion and accurately depicts changes of the collagenous microarchitecture of the AF	• DWI/DTI can capture earlier alterations of water diffusion due to premature NP dehydration and/or AF lamellar disruption	[11,17,29,35]
UTE	• Produces pulse sequences with echo times 100 −1000 times shorter than conventional sequences, thus allowing to capture CEP morphology • Can detect CEP damage, Modic changes and a specific radiological sign (UDS) associated with CEP calcification and LBP	• UTE sequences are able to thoroughly analyze CEP structure	[9,27,36,40,42,43,45]

Table 3 (***Continued***)

MRI sequence	Specific features	Advantages over traditional MRI	Relevant references
gagCEST	• Measures the chemical exchange of hydroxyl-protons between GAG and bulk water molecules, which is indicative of the IVD GAG content • Able to discriminate between the different structural features of the NP and AF • Has shown higher discrimination accuracy compared to T2*, T1ρ and diffusion imaging	• gagCEST can detect early biochemical changes in the IVD extracellular matrix before structural alterations occur	[13,28,32,35,47]
MRS	• Can detect several metabolites that may serve as IDD biomarkers (eg, alanine, collagen, LA, and PG) • Has shown to successfully recognize painful IVDs and correlate with pain and disability scores • Patients operated at levels characterized by high catabolic biomarker concentrations showed better postoperative outcomes	• MRS may provide a functional measurement of IDD biomarkers and help understand IDD pathophysiology	[8,19]
^{23}Na-MRI	• Can estimate the NP content of ^{23}Na, which is proportional to the amount of PG • Has been shown to correlate with Pfirrmann and modified Pfirrmann scores • ^{23}Na content seems to be higher in women compared to men in healthy conditions	• ^{23}Na-MRI can produce a quantitative analysis of subtle biochemical changes in the setting of IDD	[14,25]
IDEAL	• Consents to quantify the fat fraction of both vertebral bone marrow (BMFF) and paraspinal muscles • Increased paraspinal fat fraction and BMFF have been associated with worse ODI and VAS scores in patients with LBP	• IDEAL sequences are able to quantitatively describe fatty infiltration of paraspinal muscles and vertebral bodies	[9,46]
CSE-MRI	• Allows the assessment of BMFF, which is negatively correlated with the amount of hematopoietic marrow, thus providing a proxy for perfusion • Has been inversely associated with NP PG content and degeneration	• CSE-MRI can accurately describe vertebral bone marrow fat content	[40]

^{23}Na, positively charged 23 sodium; AF, annulus fibrosus; BMFF, bone marrow fat fraction; CEP, cartilaginous end plate; CSE-MRI, chemical shift encoding-based water-fat MRI; DTI, diffusion tensor imaging; DWI, diffusion-weighted imaging; GAG, glycosaminoglycan; gagCEST, glycosaminoglycan chemical exchange saturation transfer; Gd, gadolinium; IDD, intervertebral disc degeneration; IDEAL, Iterative Decomposition of water and fat with Echo Asymmetry and Least-Squares Estimation; IVD, intervertebral disc; LA, lactic acid; LBP, low back pain; LFJ, lumbar facet joints; MRS, magnetic resonance spectroscopy; NP, nucleus pulposus; ODI, Oswestry disability index; PG, proteoglycan; PD, provocative discography; qMRI, quantitative magnetic resonance imaging; UDS, ultrashort echo time disc sign; UTE, ultrashort echo time; VAS, visual analog scale.

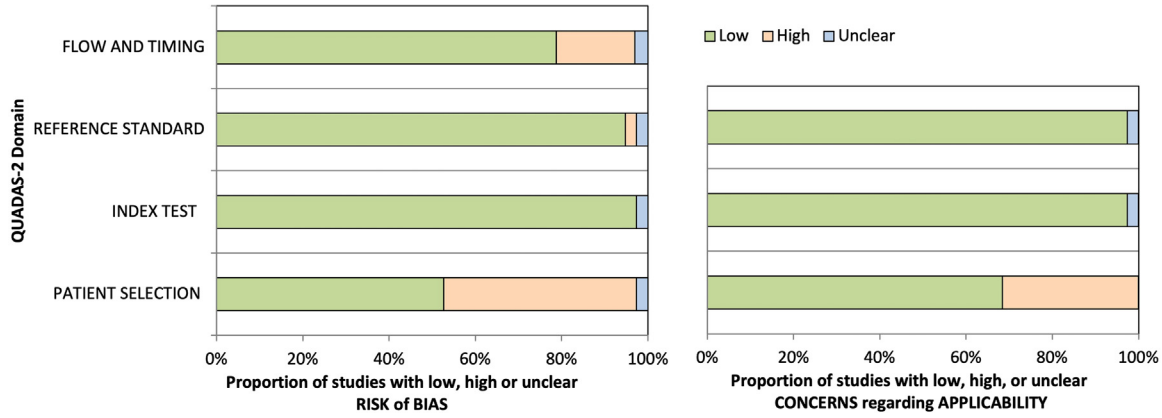

Fig. 2. Summary of the methodological quality of included studies regarding the 4 domains assessing the risk of bias (A) and the 3 domains assessing applicability concerns (B) of the QUADAS-2 score. Studies with a low risk of bias are highlighted in green, studies with an unclear risk of bias are depicted in blue and studies with a high risk of bias are represented in orange.

Pfirrmann grade in both LBP patients and controls, although results were statistically significant between groups for grade three only. When analyzing all subjects, the water/PG peak area ratio was significantly different in patients versus controls. In addition, the regression model demonstrated a significant correlation between T1ρ and the water/PG peak area ratio. Among LBP patients, IVDs with a positive PD showed a significantly higher water/PG peak area ratio compared with PD-negative IVDs. Furthermore, an increased water/PG peak area ratio was significantly associated with worse outcomes at ODI and SF-36. Gornet et al. [8] performed a prospective study on patients affected by LBP that underwent MRS of selected lumbar IVDs, whose 44% subsequently received PD. MRS generated spectral features of carbohydrate/collagen (CA) and PG as structural markers and alanine (AL), lactic acid (LA) and propionate as acidic pain markers. These components were combined to generate an MRS-SCORE for each IVD, which was directly proportional to the degree of IDD. Furthermore, averaged PG spectral measurements were used to calculate a PG-SCORE, which resulted in significant differences between Pfirrmann grades, except for grade 1 versus 2. MRS-SCOREs were significantly higher in painful IVDs compared to non-painful IVDs as well as in PD-positive IVDs compared to PD-negative IVDs. Subsequently, 89 patients from the initial cohort underwent surgery at painful IVD levels independently of MRS-SCOREs. At 6 and 12 months, patients operated at levels classified as positive at MRS ("MRSmatch") showed significantly better ODI and VAS scores compared to patients operated at levels considered negative at MRS ("MRSmiss)." Consequently, treatment success was 94% in MRSmatch patients compared to 55% in the MRSmiss group. When patients were treated at all MRS+ levels success rate reached 97%, while it dropped to 54% in patients left with an untreated MRS+ IVD.

^{23}Na-MRI

In the study by Haneder et al. [14], the mean normalized ^{23}Na signal ($^{23}Na_{norm}$) was significantly reduced in IVDs rated with Pfirrmann scores of 4 and 5 compared with Pfirrmann scores of 1 to 3 in healthy subjects. In LBP patients, significant reductions in $^{23}Na_{norm}$ were observed among IVDs with Pfirrmann scores 2 and 4 versus 5 but not relative to Pfirrmann score 3. No significant difference was found in terms of $^{23}Na_{norm}$ in individuals with the same Pfirrmann scores and no correlation was reported with age or BMI. Interestingly, mean $^{23}Na_{norm}$ was significantly higher in women compared to men, but only within the control group. In their healthy cohort, Noebauer-Huhmann et al. [25] found a cubic function at ^{23}Na-MRI between normalized sodium signal intensities and modified Pfirrmann score. Interestingly, the Pearson coefficient showed no correlation between normalized sodium signal intensities and T2. Furthermore, no significant difference in sodium signal was noticed among different levels and with regard to patients' age.

IDEAL

In their study, Bailey et al. [9] acquired IDEAL sequences for paraspinal muscle fat fraction measurement in patients with chronic LBP and matched asymptomatic individuals. Interestingly, patients with greater disability (ODI>40) showed a significantly increased fat fraction within the paraspinal muscles, which was also associated with a higher risk of CEP damage at L4−L5.

On the other hand, Krug et al. [46] performed IDEAL MRI to evaluate vertebral BMFF as an index of hematopoietic bone marrow conversion to the significantly less perfused yellow bone marrow. The authors showed that BMFF was significantly associated with VAS and ODI scores in patients with LBP and inversely correlated with both IVD T1ρ and T2 values, especially at L4-L5 and L5-S1 levels.

CSE-MRI

In the study from Bonnheim et al. [40], CSE-MRI showed that vertebral BMFF was independently and significantly associated with T1ρ and age, but not after adjusting for age, sex, and BMI. Furthermore, the multivariate model showed that BMFF was not able to predict NP T1ρ and demonstrated that the relationship between NP T1ρ and CEP T2* did not depend on vertebral BMFF.

Discussion

Advanced qMRI techniques aimed at investigating IDD have been rapidly evolving in recent years [4,48]. The common endpoint of all these tools is to capture the degenerative process occurring within the IVDs as soon as possible. Ideally, advanced MRI techniques are implemented and adjusted to detect IDD before the drop of T2 signal intensity, which is one of the earliest signs that can be observed with conventional MRI [49,50]. To this end, various strategies have been attempted with different results. The first notable difference among MRI tools for the analysis of IDD concerns the use of gadolinium-based contrast agents (GBCAs), such as delayed gadolinium enhancement in T1 mapping [24]. Indeed, GBCAs are injected intravenously to shorten T1 relaxation times of tissues with gadolinium absorption [51]. Despite interesting and statistically significant results reported by the authors [24], it is known that the injection of GBCAs usually increases scanning time and should be avoided if similar results can be achieved with MRI sequences obtained without GBCAs. Indeed, several other MRI sequences to investigate IDD do not require the use of GBCAs.

T2 mapping, for instance, is basedon T2 relaxation time of tissues and allows to build maps to measure PG, water, and collagen anisotropy within IVDs [52]. On the other hand, T1ρ mapping relies on T1 relaxation time, it is achieved with the so-called spin-lock MRI and mirrors the slow interactions between ECM macromolecules and bulk water [53]. Although T1ρ sequences showed more sensitivity with respect to T2 in evaluating IVD hydration and PG content at early stages of degeneration, they require an additional radiofrequency (RF) pulse resulting in higher specific absorption rates (SAR) [54]. Moreover, quantitative T2* mapping also showed some advantages over T2 mapping, including three-dimensionality, shorter acquisition times, and greater signal-to-noise ratio, together with the drawbacks related to the influence of cartilage orientation and requirement of high-field strengths and high RF energy levels [34,55]. Overall, T1ρ, T2 and T2* mapping have shown to significantly correlate with advancing IDD as per the Pfirrmann classification as well as among each other, with some studies also specifically reporting lower values in patients with LBP or disc herniation [10,11,15,19,21,22,41,46].

Another approach being tested for noninvasive imaging of IDD is diffusion MRI. DWI and DTI allow to obtain measures of water molecular diffusion, indirectly providing information on tissue microstructural composition and organization [17,56,57]. Indeed, diffusion imaging has been demonstrated to effectively capture the reduction of water content in lumbar IVDs due to IDD in patients with LBP and disc herniation [11,17,35]. However, these promising markers of IVD integrity are prone to motion artifacts and hold challenges due to the balance of signal-to-noise [17,56,57].

MRI UTE sequence is achieved by adjusting echo time (TE) <1 ms, allowing to measure signals from tissues with short T2 properties [58], whereas MRS yields quantitative tissue samples of metabolite levels as well as their spatial distribution in specific ROIs [59]. Both these tools have shown promising results but are limited by motion artifacts, scanning times, and availability [58,59]. GagCEST imaging quantifies GAG and bulk water content basedon the exchange of hydroxyl protons [60,61]. The main drawbacks of gagCEST are reduced signal-to-noise ratio (SNR) and difficult discrimination between frequencies of hydroxyl-GAG and water. These issues may be mitigated by using 7 Tesla MRI scanners, which are considerably expensive and thus difficult to apply on a larger scale [60,61].

Moreover, ^{23}Na-MRI is another option to quantify sodium concentration which is an indicator of GAG/PG tissue content and, therefore, has been utilized to assess ECM changes within degenerating IVDs [62]. Three and 7 Tesla magnetic field scanners have been suggested to account for the weaknesses of ^{23}Na-MRI technique providing lower relaxation times, with respect to proton imaging, low SNR, and a low gyromagnetic ratio [62].

A different approach involves assessing paraspinal tissues to acquire predictive information on IDD using body composition imaging [63−65]. Very intriguing results have been reported by Bailey et al. [9] using IDEAL sequences for paraspinal muscle fat fraction measurement. Indeed, increased paravertebral muscle fatty infiltration and poor function may lead to compromised spinal alignment and impaired biomechanics, which may in turn increase load transmission and microtrauma within IVDs. Nonetheless, increased vertebral body BMFF assessed with both IDEAL sequences [46] and CSE-MRI [40] has also been associated with advancing IDD possibly due to reduced vertebral perfusion, consequently hindering nutrient diffusion through the end plates towards the IVDs.

Despite interesting and promising available MRI tools to investigate IDD, there is no consensus on the best imaging solution. Further effort will be needed to validate and standardize imaging strategies in this context and to translate them into routine clinical practice. It is likely that multimodal imaging integrating multiple techniques and matching IVDs with paraspinal soft tissues will be the key to improving the current standard of care.

This study has some limitations. First, significant heterogeneity across studies in terms of included populations, MRI sequences, as well as the absence of patient-related outcomes prevented a meta-analysis to be performed.

Second, the overall quality of data was considerably low due to the absence of controlled studies, both randomized and nonrandomized. Third, as the search included English manuscripts only, we may have missed articles written in other languages matching our inclusion criteria.

Conclusions

The aim of this study was to systematically review the available evidence on innovative MRI tools for the early diagnosis of IDD. Most included studies were preliminary in nature and performed on small cohorts. However, the techniques used demonstrated to effectively detect early degenerative changes compared to conventional MRI. Further studies are needed to validate these novel technologies in terms of applicability, cost-effectiveness, and possible role as game changers in the care of LBP.

Declarations of Competing Interests

The authors declare that they have no known competing financial interests or personal relationships that could have appeared to influence the work reported in this paper.

Supplementary materials

Supplementary material associated with this article can be found in the online version at https://doi.org/10.1016/j.spinee.2023.05.011.

References

[1] Russo F, De Salvatore S, Ambrosio L, Vadalà G, Fontana L, Papalia R, et al. Does workers' compensation status affect outcomes after lumbar spine surgery? a systematic review and meta-analysis. Int J Environ Res Public Health 2021;18(11):6165.
[2] Knezevic NN, Candido KD, Vlaeyen JWS, Van Zundert J, Cohen SP. Low back pain. The Lancet 2021;398(10294):78–92.
[3] Taher F, Essig D, Lebl DR, Hughes AP, Sama AA, Cammisa FP, et al. Lumbar degenerative disc disease: current and future concepts of diagnosis and management. Adv Orthop 2012;2012:970752.
[4] Mallio CA, Vadalà G, Russo F, Bernetti C, Ambrosio L, Zobel BB, et al. Novel magnetic resonance imaging tools for the diagnosis of degenerative disc disease: a narrative review. Diagnostics 2022;12(2).
[5] Urban JP, Winlove CP. Pathophysiology of the intervertebral disc and the challenges for MRI. J Magn Reson Imaging 2007;25(2):419–32.
[6] Page MJ, Moher D, Bossuyt PM, Boutron I, Hoffmann TC, Mulrow CD, et al. PRISMA 2020 explanation and elaboration: updated guidance and exemplars for reporting systematic reviews. BMJ 2021;372:n160.
[7] Whiting PF, Rutjes AW, Westwood ME, Mallet S, Deeks JJ, Reitsma JB, et al. QUADAS-2: a revised tool for the quality assessment of diagnostic accuracy studies. Ann Intern Med 2011;155(8):529–36.
[8] Gornet MG, Peacock J, Claude J, Schranck FW, Copay AG, Eastlack RK, et al. Magnetic resonance spectroscopy (MRS) can identify painful lumbar discs and may facilitate improved clinical outcomes of lumbar surgeries for discogenic pain. Eur Spine J 2019;28(4):674–87.
[9] Bailey JF, Fields AJ, Ballatori A, Cohen D, Jain D, Coughlin D, et al. The Relationship between endplate pathology and patient-reported symptoms for chronic low back pain depends on lumbar paraspinal muscle quality. Spine (Phila Pa 1976) 2019;44(14):1010–7.
[10] Borthakur A, Maurer PM, Fenty M, Wang C, Berger R, Yoder J, et al. T1rho magnetic resonance imaging and discography pressure as novel biomarkers for disc degeneration and low back pain. Spine (Phila Pa 1976) 2011;36(25):2190–6.
[11] Cui YZ, Yang XH, Liu PF, Wang B, Chen WJ. Preliminary study on diagnosis of lumbar disc degeneration with magnetic resonance T1p, T2 mapping and DWI quantitative detection technologies. Eur Rev Med Pharmacol Sci 2016;20(16):3344–50.
[12] Deng M, Yuan J, Chen WT, Chan Q, Griffith JF, Wang YX. Evaluation of glycosaminoglycan in the lumbar disc using chemical exchange saturation transfer mr at 3.0 tesla: reproducibility and correlation with disc degeneration. Biomed Environ Sci 2016;29(1):47–55.
[13] Frenken M, Nebelung S, Schleich C, Müller-Lutz A, Radke KL, Kamp B, et al. Non-specific low back pain and lumbar radiculopathy: comparison of morphologic and compositional MRI as assessed by gagCEST imaging at 3T. Diagnostics (Basel) 2021;11(3).
[14] Haneder S, Ong MM, Budjan JM, Schmidt R, Konstandin S, Morelli JN, et al. 23Na-magnetic resonance imaging of the human lumbar vertebral discs: in vivo measurements at 3.0 T in healthy volunteers and patients with low back pain. Spine J 2014;14(7):1343–50.
[15] Ogon I, Takebayashi T, Takashima H, Tanimoto K, Ida K, Yoshimoto M, et al. Analysis of chronic low back pain with magnetic resonance imaging T2 mapping of lumbar intervertebral disc. J Orthop Sci 2015;20(2):295–301.
[16] Vadala G, Russo F, Battisti S, Stellato L, Martina F, Del Vescovo R, et al. Early intervertebral disc degeneration changes in asymptomatic weightlifters assessed by t1rho-magnetic resonance imaging. Spine (Phila Pa 1976) 2014;39(22):1881–6.
[17] Vadapalli R, Mulukutla R, Vadapalli AS, Vedula RR. Quantitative predictive imaging biomarkers of lumbar intervertebral disc degeneration. Asian Spine J 2019;13(4):527–34.
[18] Wang Y-XJ, Griffith JF, Leung JCS, Yuan J. Age related reduction of T1rho and T2 magnetic resonance relaxation times of lumbar intervertebral disc. Quantit Imaging Med Surg 2014;4(4):259–64.
[19] Zuo J, Joseph GB, Li X, Link TM, Hu SS, Berven SH, et al. In vivo intervertebral disc characterization using magnetic resonance spectroscopy and T1rho imaging: association with discography and Oswestry Disability Index and Short Form-36 Health Survey. Spine (Phila Pa 1976) 2012;37(3):214–21.
[20] Auerbach JD, Johannessen W, Borthakur A, Wheaton AJ, Dolinskas CA, Balderston RA, et al. In vivo quantification of human lumbar disc degeneration using T(1rho)-weighted magnetic resonance imaging. Eur Spine J 2006;15(Suppl 3):S338–44.
[21] Blumenkrantz G, Zuo J, Li X, Kornak J, Link TM, Majumdar S. In vivo 3.0-tesla magnetic resonance T1rho and T2 relaxation mapping in subjects with intervertebral disc degeneration and clinical symptoms. Magn Reson Med 2010;63(5):1193–200.
[22] Hoppe S, Quirbach S, Mamisch TC, Krause FG, Werlen S, Benneker LM. Axial T2 mapping in intervertebral discs: a new technique for assessment of intervertebral disc degeneration. Eur Radiol 2012;22(9):2013–9.
[23] Menezes-Reis R, Salmon CE, Bonugli GP, Mazoroski D, Tamashiro MH, Savarese LG, et al. Lumbar intervertebral discs T2 relaxometry and T1rho relaxometry correlation with age in asymptomatic young adults. Quant Imaging Med Surg 2016;6(4):402–12.
[24] Niinimaki JL, Parviainen O, Ruohonen J, Ojala RO, Kurunlahti M, Karppinen J, et al. In vivo quantification of delayed gadolinium enhancement in the nucleus pulposus of human intervertebral disc. J Magn Reson Imaging 2006;24(4):796–800.
[25] Noebauer-Huhmann IM, Juras V, Pfirrmann CW, Szolomanyi P, Zbyn S, Messner A, et al. Sodium MR imaging of the lumbar intervertebral disk at 7 T: correlation with T2 mapping and modified Pfirrmann score at 3 T−preliminary results. Radiology 2012;265(2):555–64.

[26] Pandit P, Talbott JF, Pedoia V, Dillon W, Majumdar S. T1rho and T2 -based characterization of regional variations in intervertebral discs to detect early degenerative changes. J Orthop Res 2016;34(8):1373–81.
[27] Pang H, Bow C, Cheung JPY, Zehra U, Borthakur A, Karppinen J, et al. The UTE disc sign on MRI: a novel imaging biomarker associated with degenerative spine changes, low back pain, and disability. Spine (Phila Pa 1976) 2018;43(7):503–11.
[28] Schleich C, Muller-Lutz A, Eichner M, Scmitt B, Matuschke F, Bittersohl B, et al. Glycosaminoglycan chemical exchange saturation transfer of lumbar intervertebral discs in healthy volunteers. Spine (Phila Pa 1976) 2016;41(2):146–52.
[29] Shen S, Wang H, Zhang J, Wang F, Liu SR. Diffusion weighted imaging, diffusion tensor imaging, and T2* mapping of lumbar intervertebral disc in young healthy adults. Iran J Radiol 2016;13(1):e30069.
[30] Stelzeneder D, Welsch GH, Kovacs BK, Goed S, Paternostro-Sluga T, Vlychou M, et al. Quantitative T2 evaluation at 3.0T compared to morphological grading of the lumbar intervertebral disc: a standardized evaluation approach in patients with low back pain. Eur J Radiol 2012;81(2):324–30.
[31] Takashima H, Takebayashi T, Yoshimoto M, Terashima Y, Tsuda H, Ida K, et al. Correlation between T2 relaxation time and intervertebral disk degeneration. Skeletal Radiol 2012;41(2):163–7.
[32] Togao O, Hiwatashi A, Wada T, Yamashita K, Kikuchi K, Tokunaga C, et al. A qualitative and quantitative correlation study of lumbar intervertebral disc degeneration using glycosaminoglycan chemical exchange saturation transfer, Pfirrmann grade, and T1-rho. AJNR Am J Neuroradiol 2018;39(7):1369–75.
[33] Watanabe A, Benneker LM, Boesch C, Watanabe T, Obata T, Anderson SE. Classification of intervertebral disk degeneration with axial T2 mapping. AJR Am J Roentgenol 2007;189(4):936–42.
[34] Welsch GH, Trattnig S, Paternostro-Sluga T, Bohndorf K, Goed S, Stelzeneder D, et al. Parametric T2 and T2* mapping techniques to visualize intervertebral disc degeneration in patients with low back pain: initial results on the clinical use of 3.0 Tesla MRI. Skeletal Radiol 2011;40(5):543–51.
[35] Xiong X, Zhou Z, Figini M, Shangguan J, Zhang Z, Chen W. Multiparameter evaluation of lumbar intervertebral disc degeneration using quantitative magnetic resonance imaging techniques. Am J Transl Res 2018;10(2):444–54.
[36] Zehra U, Bow C, Cheung JPY, Pang H, Lu W, Samartzis D. The association of lumbar intervertebral disc calcification on plain radiographs with the UTE Disc Sign on MRI. Eur Spine J 2018;27(5):1049–57.
[37] Zhang X, Yang L, Gao F, Yuan Z, Lin X, Yao B, et al. Comparison of T1rho and T2* relaxation mapping in patients with different grades of disc degeneration at 3T MR. Med Sci Monit 2015;21:1934–41.
[38] Zhang Y, Hu J, Duan C, Hu P, Lu H, Peng X. Correlation study between facet joint cartilage and intervertebral discs in early lumbar vertebral degeneration using T2, T2* and T1rho mapping. PLoS One 2017;12(6):e0178406.
[39] Zobel BB, Vadala G, Del Vescovo R, Battisti S, Martina FM, Stellato L, et al. T1rho magnetic resonance imaging quantification of early lumbar intervertebral disc degeneration in healthy young adults. Spine (Phila Pa 1976) 2012;37(14):1224–30.
[40] Bonnheim NB, Wang L, Lazar AA, Zhou J, Chachad R, Sollmann N, et al. The contributions of cartilage endplate composition and vertebral bone marrow fat to intervertebral disc degeneration in patients with chronic low back pain. Eur Spine J 2022;31(7):1866–72.
[41] Yang L, Sun C, Gong T, Li Q, Chen X, Zhang X. T1rho, T2 and T2* mapping of lumbar intervertebral disc degeneration: a comparison study. BMC Musculoskelet Disord 2022;23(1):1135.
[42] Wu LL, Liu LH, Rao SX, Wu PY, Zhou JJ. Ultrashort time-to-echo T2* and T2* relaxometry for evaluation of lumbar disc degeneration: a comparative study. BMC Musculoskelet Disord 2022;23(1):524.
[43] Wei Z, Lombardi AF, Lee RR, Wallace M, Masuda K, Chang EY, et al. Comprehensive assessment of in vivo lumbar spine intervertebral discs using a 3D adiabatic T(1rho) prepared ultrashort echo time (UTE-Adiab-T(1rho)) pulse sequence. Quant Imaging Med Surg 2022;12(1):269–80.
[44] Lagerstrand K, Brisby H, Hebelka H. Associations between high-intensity zones, endplate, and Modic changes and their effect on T2-mapping with and without spinal load. J Orthopaed Res 2021;39(12):2703–10.
[45] Takashima H, Yoshimoto M, Ogon I, Takebayashi T, Imamura R, Akatsuka Y, et al. T1rho, T2, and T2* relaxation time based on grading of intervertebral disc degeneration. Acta Radiologica 2022;64 (3):1116–21.
[46] Krug R, Joseph GB, Han M, Fields A, Cheung J, Mundada M, et al. Associations between vertebral body fat fraction and intervertebral disc biochemical composition as assessed by quantitative MRI. J Magn Reson Imaging 2019;50(4):1219–26.
[47] Deng Y, Scherer PE. Adipokines as novel biomarkers and regulators of the metabolic syndrome. Ann N Y Acad Sci 2010;1212:E1–E19.
[48] Tamagawa S, Sakai D, Nojiri H, Sato M, Ishijima M, Watanabe M. Imaging evaluation of intervertebral disc degeneration and painful discs—Advances and challenges in quantitative MRI. Diagnostics 2022;12(3).
[49] Pfirrmann CW, Metzdorf A, Zanetti M, Hodler J, Boos N. Magnetic resonance classification of lumbar intervertebral disc degeneration. Spine (Phila Pa 1976) 2001;26(17):1873–8.
[50] Griffith JF, Wang YX, Antonio GE, Choi KC, Yu A, Ahuja AT, et al. Modified Pfirrmann grading system for lumbar intervertebral disc degeneration. Spine (Phila Pa 1976) 2007;32(24):E708–12.
[51] Mallio CA, Lo Vullo G, Messina L, Beomonte Zobel B, Parizel PM, Quattrocchi CC. Increased T1 signal intensity of the anterior pituitary gland on unenhanced magnetic resonance images after chronic exposure to gadodiamide. Invest Radiol 2020;55(1):25–9.
[52] Wang C, Auerbach JD, Witschey WR, Balderston RA, Reddy R, Borthakur A. Advances in Magnetic Resonance Imaging for the assessment of degenerative disc disease of the lumbar spine. Semin Spine Surg 2007;19(2):65–71.
[53] Yoon MA, Hong SJ, Kang CH, Ahn KS, Kim BH. T1rho and T2 mapping of lumbar intervertebral disc: correlation with degeneration and morphologic changes in different disc regions. Magn Reson Imaging 2016;34(7):932–9.
[54] Wang YX, Zhang Q, Li X, Chen W, Ahuja A, Yuan J. T1rho magnetic resonance: basic physics principles and applications in knee and intervertebral disc imaging. Quant Imaging Med Surg 2015;5 (6):858–85.
[55] Huang L, Liu Y, Ding Y, Wu X, Zhang N, Lai Q, et al. Quantitative evaluation of lumbar intervertebral disc degeneration by axial T2* mapping. Medicine (Baltimore) 2017;96(51):e9393.
[56] Kealey SM, Aho T, Delong D, Barboriak DP, Provenzale JM, Eastwood JD. Assessment of apparent diffusion coefficient in normal and degenerated intervertebral lumbar disks: initial experience. Radiology 2005;235(2):569–74.
[57] Wu N, Liu H, Chen J, Zhao L, Zuo W, Ming Y, et al. Comparison of apparent diffusion coefficient and T2 relaxation time variation patterns in assessment of age and disc level related intervertebral disc changes. PLoS One 2013;8(7):e69052.
[58] Ogon I, Takebayashi T, Takashima H, Morita T, Terashima Y, Yoshimoto M, et al. Imaging diagnosis for intervertebral disc. JOR Spine 2020;3(1):e1066.
[59] de Mello R, Ma Y, Ji Y, Du J, Chang EY. Quantitative MRI musculoskeletal techniques: an update. AJR Am J Roentgenol 2019;213 (3):524–33.
[60] Schleich C, Lutz A, Schmitt B, Wittsack H-J, Miese FR. Magnetic resonance gagCEST imaging of the human lumbar intervertebral disc: age dependency of glycosaminoglycan content. In: Radiological Society of North America 2014 Scientific Assembly and Annual Meeting; 2014.
[61] Banjar M, Horiuchi S, Gedeon DN, Yoshioka H. Review of quantitative knee articular cartilage MR imaging. Magn Reson Med Sci 2021;21 (1):29–40.

[62] Zaric O, Juras V, Szomolanyi P, Schreiner M, Raudner M, Giraudo C, et al. Frontiers of sodium MRI revisited: from cartilage to brain imaging. J Magn Reson Imaging 2021;54(1):58–75.

[63] Quattrocchi CC, Giona A, Di Martino A, Gaudino F, Mallio CA, Errante Y, et al. Lumbar subcutaneous edema and degenerative spinal disease in patients with low back pain: a retrospective MRI study. Musculoskelet Surg 2015;99(2):159–63.

[64] Greco F, Quarta LG, Grasso RF, Beomonte Zobel B, Mallio CA. Increased visceral adipose tissue in clear cell renal cell carcinoma with and without peritumoral collateral vessels. Br J Radiol 2020;93 (1112).

[65] Greco F, Mallio CA, Grippo R, Messina L, Vallese S, Rabitti C, et al. Increased visceral adipose tissue in male patients with non-clear cell renal cell carcinoma. La Radiol Med 2020;125(6):538–43.